WEIGHTED CENTROID METHOD FOR BREAST TUMOR LOCALIZATION USING AN UWB RADAR

A. Lazaro, D. Girbau, and R. Villarino

Department of Electronics, Electrics and Automatics Engineering
Universitat Rovira i Virgili (URV)
Av. Països Catalans 26, Campus Sescelades, 43007 Tarragona, Spain

Abstract—This paper studies the potential of ultra-wideband (UWB) microwave imaging for detection and localization of breast cancer in its early stages. A method is proposed for locating tumors which is based on the time-of-flight of the signal backscattered at the tumor. Time-of-flight is detected using a wavelet transform algorithm. The main contribution of this paper is that it proposes to determine the position of the tumor by using an adapted version of the centroid localization method used in wireless sensor nodes. Its main advantage is that it does not require knowing a priori neither the propagation velocity of the breast nor its dielectric permittivity. The feasibility of the method has been investigated by means of simulated and experimental results with an ultra-wideband radar and a phantom.

1. INTRODUCTION

In recent years, microwave breast tumor detection is growing as a promising technique [1–10], since it is a non-invasive technique that uses non-ionizing radiation. It is considered a potential alternative or complement to X-rays [1, 2], which is the basic technique used in breast cancer detection today. Measured data available at the literature shows an important contrast in the dielectric properties between malign and normal breast tissues [1], and this is the basis for microwave breast imaging.

Current research focuses on two categories, microwave tomography [6–8] and ultra-wideband (UWB) radar-based approach [1–5]. In the latter, several techniques have recently been developed — Concepts and circuits based on UWB pulses, especially for communication

systems [11], which have also proved interesting for tomography applications. In consequence a number of imaging methods for UWB microwave imaging of breast tumors are already available [1–5]. Most of them are based on focusing techniques such as delay-and-sum [1]. In these techniques an image of the backscattered signal is obtained by time-shifting the received signals in order to align the returns from a focal point and then the waveforms for all the antennas are added. The process is repeated scanning the breast. Alternative techniques are based on a high-resolution UWB radar that uses sub-nanosecond pulses to illuminate the scene [9, 10, 12, 13]. If there is an object in the illumination area, a part of the transmitted pulse will be reflected and detected by the receiver. In these techniques the objective is the localization of the tumor position assuming that it causes the strongest backscatter.

In recent years, several localization systems using UWB technology have been implemented [14]. In these systems, ranges are determined between the object and the known points by measuring the time-of-flight (or time-of-arrival, ToA) of a UWB signal between a transmitter and a receiver (located at known positions). The ranges are obtained by multiplying the measured time-of-flight by the speed of light. Unfortunately, in the case of breast cancer detection using UWB, the reflected pulses are contaminated by noise and undesired reflections at other objects which increase the clutter level. The classic approach to estimate ToA consists in the correlation-based ToA estimation or matched-filter [15]. In this approach the estimation of ToA is obtained from the time shift of a template signal that produces the maximum correlation with the received signal. A matched-filter time reversal approach has been proposed in [9] for breast cancer detection, where only FDTM simulated results were presented. It is known that the matched filter is the optimum detector if the shape of the pulse is known. However, in breast cancer detection, the transmitted waveform cannot be used as template because the backscattered pulse at the tumor is propagated through the breast, with different permittivity than air. In consequence, the reflected pulses are distorted due to the change in medium velocity and its propagation in a dispersive medium. This problem can be mitigated by using a coupling medium [16] (for instance, fat) to avoid reflections in the skin and then pulses propagate in a homogeneous-like medium. However, the problem here is that the UWB antennas must be designed to operate immersed in this lossy coupling material. Moreover, the dielectric constant of fat has a great variability among women [1, 17]. In practice, it is not easy to choose a template signal to apply the matched-filter or correlation technique.

In order to solve this drawback, the authors proposed in [10] a

technique to estimate the ToA based on a wavelet decomposition of the backscattered signals. When the transmitted pulse hits the breast surface, a portion is backscattered towards the receiver and a portion propagates inside the breast and hits in reflecting objects such as a region of tumor tissue. These reflected pulses can be separated due to the high resolution of UWB radars but, unfortunately, their shape is not available in real UWB systems since, as stated, there are several potential sources of pulse distortion during propagation. Thus, the matched-filter technique cannot be directly applied. Therefore, the received pulse, as a first approximation, is a scaled and time-shifted version of the transmitted pulse. In order to overcome this drawback, [10] proposes to use the Continuous Wavelet Transform (CWT) as a multiscale matched filter [18–21]. The Continuous Wavelet Transform (CWT) can handle different stretched pulses, but the basic shape of the sought impulse still has to be known a priori. However, this drawback can be eliminated by using a complex extension to the signal, as well as to the wavelet, as presented in [14]. In fact, the CWT performs a correlation between the received signal and a family of scaled and time-shifted wavelets [18]. In consequence, maximum output can be expected when the input signal most resembles the wavelet template.

After identifying the reflections at the tumor for several antenna positions, its position can be located [9, 12, 13]. However, in contrast with [9, 12, 13], where only numerical results were presented and it was assumed that the breast-skin interface was perfectly matched, [10] considers air-coupled antennas (a more realistic case) and experimentally validates that technique. There, a localization technique based on least squares minimization of error between the distance of each antenna and the measured distance obtained from the pulse time-of-flight is implemented. However, in this localization method, as it is common in microwave imaging and in the time reversal method, the average fat velocity or its dielectric constant is needed. As stated before, this can be a serious drawback in clinical cases due to the great variability among women. It has been demonstrated in [10] that the minimum RMS error using the least squares is produced for values close to the real permittivity. Then, the breast permittivity is obtained from a sweep of the permittivity until a minimum in the RMS error has been found. However, this is a time-consuming technique. In this paper, a new approach is proposed. Its main advantage is that the average velocity or permittivity of the breast is not needed. The approach is inspired in a known localization method used in wireless sensor networks [22, 23], known as centroid localization method. Here, a novel weighted version of that method is proposed and applied to breast cancer detection. As in method proposed in [10], there is not

need any estimation of breast surface [24].

The paper is organized as follows. Section 2 describes the experimental setup developed to validate the proposed technique using a phantom. The basis of the measurement of ToA using the Continuous Wavelet Transform is also briefly described in this section. In Section 3, the weighted localization algorithm is presented. In Section 3, the performance of this localization algorithm is investigated by means of simulations. A study on the uncertainty in the measurement of ToA is presented and it is compared to the least squares method. In Section 4, the experimental results using an UWB radar are described. Finally, conclusions are drawn in Section 5.

2. EXPERIMENTAL SETUP AND PULSE DETECTION

The 2D experimental set-up is the same than in [10] and it is presented in Fig. 1. It is based on an UWB pulsed radar and a phantom to simulate the scene. The GZ1120ME-50EV pulse generator from Geozondas is used to generate a Gaussian monocycle pulse of 5 GHz central frequency and amplitude of ±5 V. Details on the pulse waveform are given in [25]. The pulse generator is connected to a UWB transmitter antenna (3.1–10.6 GHz frequency range). A metallic rod that emulates the tumor, immersed in an oil-filled cylindrical glass tank is used as a phantom [26, 27]. The skin is simulated using the cylindrical surface of the tank and the antennas are air coupled. Several reflections from surrounding objects are collected by the receiver antenna due to its low directivity. Measurements are performed with the transmitter and receiver antennas at a fixed position and rotating the phantom at several positions. The reflected pulses are detected by using the GZ6E sampler converter from Geozondas, which triggers the pulse generator.

The time of flight associated to reflected pulses are obtained following the procedure described in [10]. The transmitted pulse propagates by air to the breast. The pulse is also coupled between the transmitter and receiver antennas; this is partially eliminated by using an appropriate time-gating window. Later, the receiver picks up the pulses that have been reflected in the skin. Finally, the receiver measures the pulses reflected at the malignant tissue (due to its high reflectivity) and at other elements around the tumor that will be considered as clutter. The time-of-flight associated to the pulse reflected at the tumor can be calculated considering a monostatic scenario (since the two antennas are close to one another and the angle
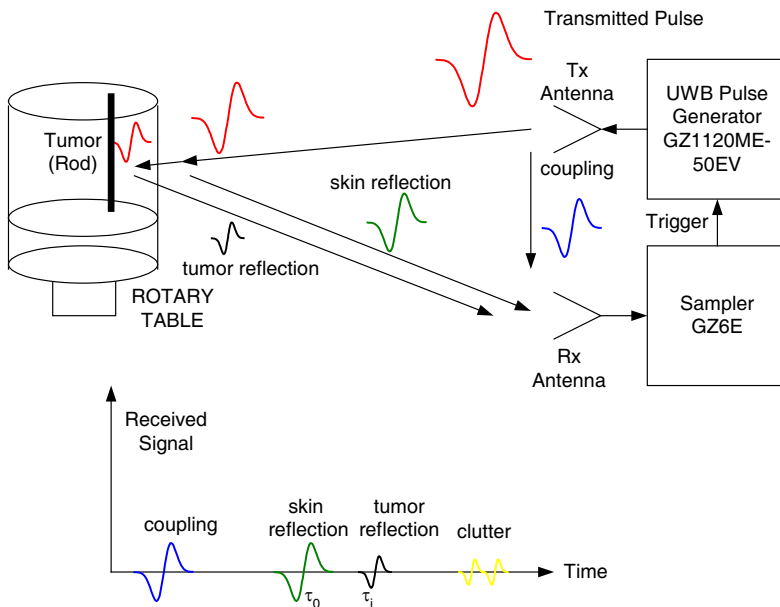
Figure 1. Experimental UWB-radar test setup.

between transmitter and receiver antennas is about 11 degrees):

$$\tau_i = \frac{2}{v}\sqrt{(x-x_i)^2 + (y-y_i)^2 + (z-z_i)^2} + \tau_{0i} + \tau_0 \qquad (1)$$

where $v = c/(\varepsilon_r)^{1/2}$ is the wave velocity in the breast, c is the vacuum light velocity, τ_{0i} is the propagation time between the antenna and the skin surface. In (1), (x, y, z) are the tumor coordinates and (x_i, y_i, z_i) are the antenna coordinates. The delay τ_0 models a systematic delay due to the cables between the transmitter and receiver and the antennas.

The determination of the tumor position requires a number of measurements for each antenna position (i) in order to obtain an undetermined system of equations with more equations than unknowns (1). In order to remove systematic clutter signals and the reflected pulses from the skin, a retrieval algorithm based on the Wiener filter described in [5] is applied. The delays, τ_{0i} and τ_i, are calculated by using the appropriate time window and detecting the peak of the magnitude of the CWT [5]. Then, the position can be graphically obtained intercepting the circles defined by (1). Alternatively, the unknown tumor position can also be obtained treating the time-of-flight system of equations as a least squares

optimization problem [10]. The non-linear model is fitted for multiple pseudoranges obtained from the positions of the known antenna points. The pseudoranges are calculated from (1):

$$\rho_i = \sqrt{(x-x_i)^2 + (y-y_i)^2 + (z-z_i)^2} = \frac{1}{2}c\left[(\tau_i - \tau_{0i})/\sqrt{\varepsilon_r} + (\tau_{0i} - \tau_0)\right] \quad (2)$$

Since in practice the propagation velocity through fat suffers great variability among persons, its permittivity (ε_r) must be considered as an unknown. A solution for this problem has been proposed in [10] using the fact that the mean error between modeled and measured range positions presents a minimum for the correct propagation velocity. Thus, an estimation of propagation velocity in fat (or permittivity) can be obtained by sweeping its value until a minimum in the error function is found. However, it is known that in iterative optimization methods the result can depend on the initial value, especially where measurement errors are present. In order to overcome these drawbacks, a new localization method for microwave breast cancer detection is proposed and described in next section.

3. WEIGTHED CENTROID LOCALISATION TECHNIQUE

In contrast to hyperbolic localization methods based on least squares optimisation method used in [10], another group of positioning algorithms has been proposed in wireless sensor networks (WSN), which are known as approximated algorithms [22, 23]. These algorithms avoid knowing the distance in their approach. One of the most popular localisation algorithms in WSN is the centroid method [22]. This algorithm has been applied in indoor environments where high multipath propagation effects are present with good performances. An adapted version for tumor localisation of the weighted centroid localization method [23] is described next.

After obtaining the time-of-arrival from the tumor reflections for all the antenna positions, the approximate position of the tumor (x, y) (assuming a 2D case due to cylindrical symmetry of the experimental setup) is estimated by a weighted centroid determination of all N positions of the antenna locations with coordinates (x_i, y_i):

$$(x, y) = \left(\frac{\sum\limits_{i=1}^{N} w_i x_i}{\sum\limits_{i=1}^{N} w_i}, \frac{\sum\limits_{i=1}^{N} w_i y_i}{\sum\limits_{i=1}^{N} w_i} \right) \quad (3)$$

where w_i is the weight between the unknown tumor position (x, y) and the antenna i with coordinates (x_i, y_i). The selection of weights is a key point in this method. The most logical choice is to set them equal to the inverse of time-of-flight within the breast:

$$w_i = \frac{1}{(\tau_i - \tau_{oi})^a} \tag{4}$$

where a (≥ 1) is an exponential smoothing factor. Then, small distances or delays due to neighbouring antennas lead to a higher weight than remote antennas with higher distances and delays (more noisy). Note that this weight choice has several advantages. First, as commented above, it does not require knowing the propagation velocity through the breast. Second, the solution does not depend on the initial value as in the optimization methods. Third, since the attenuation that suffers the signal depends on the distance, signals with longer delays experiment higher attenuations, thus their delay estimation is more difficult and the level of these signals can be masked by the clutter. Using the proposed weights (4), the contribution of these signals to (3) is smaller than the contribution of the terms from the other antennas with stronger signal and shorter delay. To this end, the smoothing factor is empirically chosen equal to 2 $(a = 2)$. For $a = 2$, the weights are proportional to the received pulse amplitudes if medium losses are ignored. Finally, the estimation of position using (3) has smaller computational complexity (i.e., matrix inversions are not required) than the least squares method.

In order to validate the proposed method a simulation to investigate the localization error is presented. Assuming a homogeneous case (for instance using a matching coupling medium) and ideal antennas located close to the skin (see Fig. 2) with coordinate positions:

$$(x_i, y_i) = (R_a \cos \phi_i, R_a \sin \phi_i) \tag{5}$$

where R_a is the antenna radius and ϕ_i is the antenna angle, the delay between the tumor and the antenna can be obtained from the following expression:

$$\tau_i = \frac{\sqrt{R_a^2 + R_t^2 - 2 R_a R_t \cos(\phi_i - \phi_t)}}{c/\sqrt{\varepsilon_r}} \tag{6}$$

where R_t is the radius of the tumor and ϕ_t its angle. Note that the most simple case is when the antennas are on the skin and $\tau_{0i} = 0$. Note also that the permittivity value is irrelevant in (3) since it appears in both the numerator and denominator and it is simplified. In the next figures a comparison between the proposed weighted centroid and the least squares methods is done.
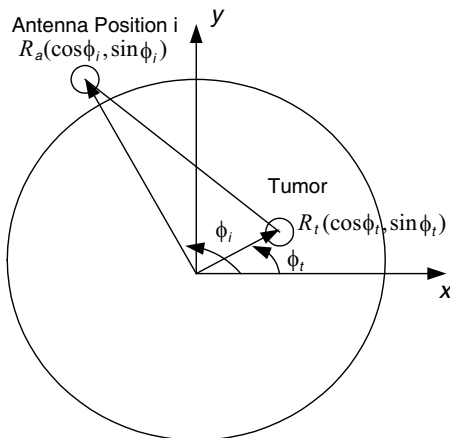
Figure 2. Schematic for position calculation.

Figure 3(a) shows the localization error using the centroid method with 8 antennas uniformly distributed as a function of the position of the tumor in a phantom with $R_a = 10\,\mathrm{cm}$. In these simulations a tumor diameter of 1 mm is assumed and the tumor position parameters R_t and ϕ_t are variable. For the same conditions, Fig. 3(b) shows the localization error using the least squares optimization method proposed in [10]. As it is shown in the Complementary Distribution Function in Fig. 4, the centroid method performs better than the least squares. This is because in the latter, the error increases when the tumor is near the skin. In these tumor locations the range to the nearest antenna is very small compared to the other antennas and, in consequence, the system matrix may be bad conditioned since some terms are inversely proportional to the ranges. This is a known drawback of gradient-based optimization methods. Moreover, in this simulation it is assumed that the propagation velocity is known. In practice, the uncertainty in the velocity will increase the localization error when the least squares method is used.

In the experimental setup (see Fig. 1), a phantom with an antenna synthetic array generated by rotating the sample is used. However, in clinical cases, a switched antenna array should be used. Then the number of antennas is limited. In order to investigate the influence of the number of antennas, Fig. 5 compares the mean localization error as a function of the number of antennas for the two localization methods. It can be concluded that the error in both methods is stabilized when 8 or more antennas are used.

Although the pulse delay detection based on CWT has great robustness in front of measurements errors, a small uncertainty in the time-of-flight can be expected. Fig. 6 shows the mean error in the localization of a tumor in the same scene as in Fig. 3, but adding a random variable to model the uncertainty in the range (or delay) determination. Again this figure shows that the centroid method is more robust to measurements errors.
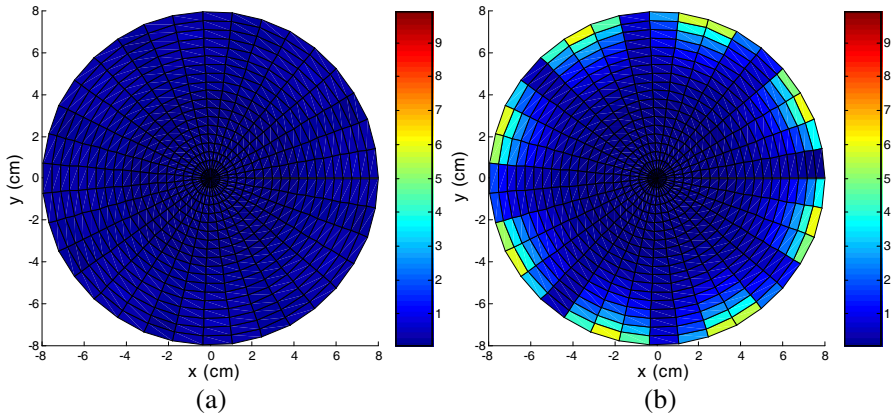

Figure 3. Localization error (in mm) using 8 antennas, (a) the centroid method, (b) least squares method.
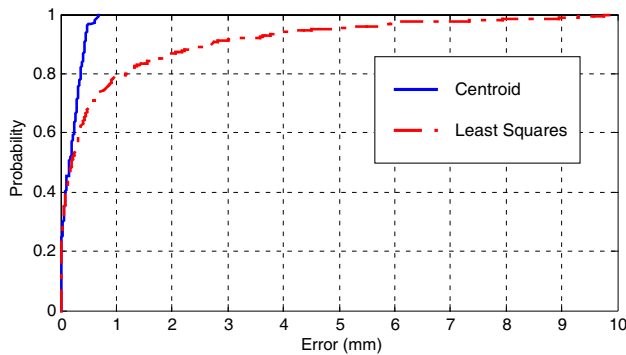

Figure 4. Comparison between the complementary distribution function for the centroid method and the least squares method using 8 antennas.
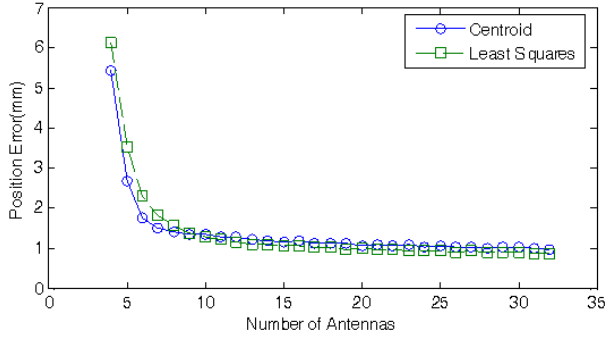
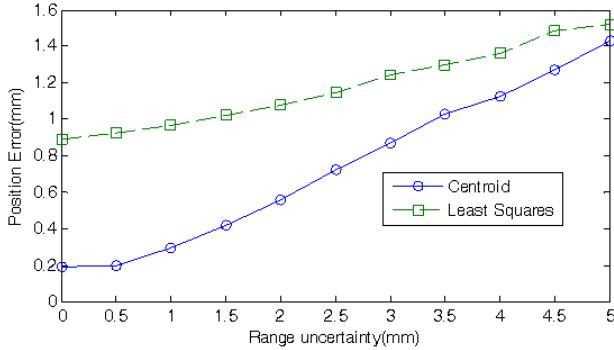**Figure 5.** Mean position error as a function of the number of antennas.

Figure 6. Mean error position using 8 antennas as a function of range uncertainty.

4. EXPERIMENTAL RESULTS

Experimental results obtained with the setup introduced in Section 2 are here presented to validate the proposed methodology. The tumor is emulated with a 0.5-cm diameter rod immersed in an oil-filled 6-cm radius methacrylate cylinder (nominal dielectric permittivities of oil and the methacrylate are 2.5 and 2.65, respectively). Fig. 7(a) shows the raw measured signals for all the antenna positions ($0°$ to $360°$, step-angle $= 2°$). Fig. 7(b) shows the signals after applying a skin retrieval algorithm based on the Wiener filter. The coupling between antennas and the backscattering signals corresponding to the cylinder surface are easily eliminated using an appropriate time window. From the observation of the time response, it is clear that the tumor information

is located between 2.5 and 3.4 ns. Fig. 8(a) plots the ToA associated to the cylinder surface (τ_{0i}), and the tumor (τ_i) for each angle. Time peaks of τ_{0i} and τ_i are obtained from the CWT explained in Section 2.
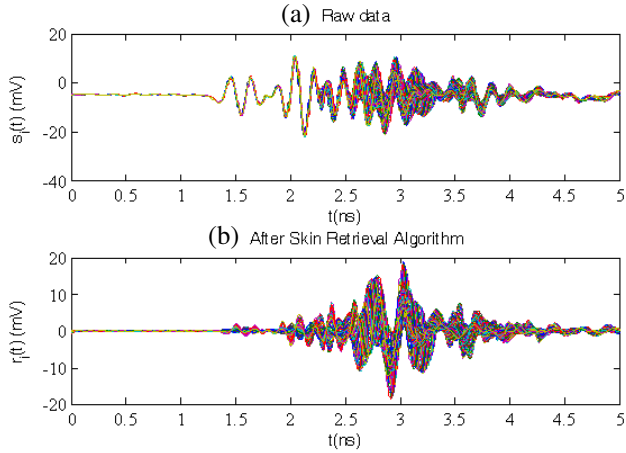
Figure 7. (a) Measured signal with the rod and (b) signal after the skin retrieval algorithm based on the Wiener filter is applied.
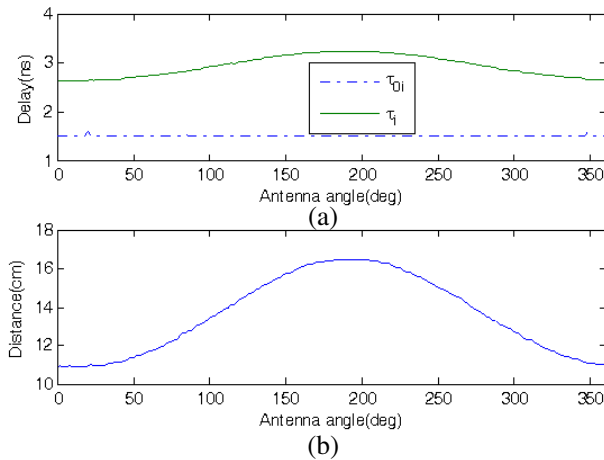
Figure 8. (a) Measured time-of-flight between antenna and cylinder surface, τ_{0i}, and between the antenna and rod, τ_i, as a function of the antenna angle and (b) distance that travels the wave that hits on the rod as a function of the angle.
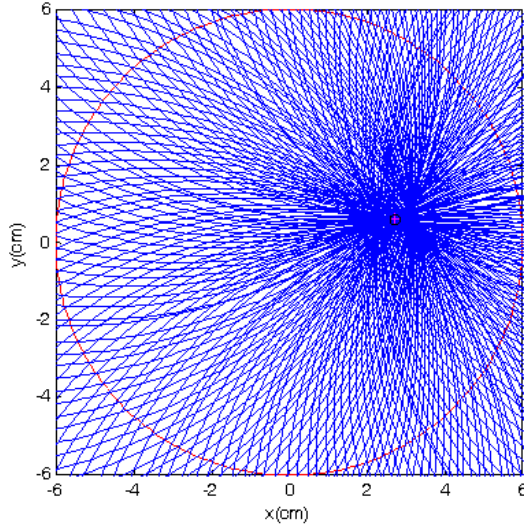
Figure 9. Interception of the circles for the tumor located at $(3\,\text{cm} <$ $12.6°)$. Position obtained by optimization $(+)$ and by the centroid method (o).

Observing the value of τ_{0i}, it is obvious that the distance between the cylinder surface and the antenna is constant. The pseudo ranges from the ToA are calculated using (2). Fig. 8(b) shows the distance that travels the wave that hits on the rod as a function of the angle. From the plot of the circles (Fig. 9) the tumor position $(3\,\text{cm} < 12.6°)$ can be determined. This position is confirmed applying the least squares optimization algorithm and the centroid algorithm. The difference in the rod position obtained for both methods is under $1\,\text{mm}$.

5. CONCLUSIONS

In this work, the viability of breast tumor detection using UWB has been investigated. In contrast to microwave breast imaging based on focusing techniques, the technique proposed in this paper is based on the localization of the tumor position using the time-of-flight of backscattered UWB pulses. Since pulses are distorted due to propagation through dispersive mediums, diffraction and multipath propagation, a detection technique based on the Continuous Wavelet Transform (CWT) has been used. The robustness of this technique in presence of noise has been proved and a procedure to determine the

pseudorange from the time-of-flight has been described. A Wiener-filter skin-breast artifact removal algorithm is used to eliminate the clutter associated with the skin and the response of the antennas. After this calibration procedure, the time-of-flight associated with the tumor reflection is obtained from the peak of the magnitude of the calibrated CWT signal. A new localization method has been proposed based on the weighted centroid localization technique. The robustness of this method has been demonstrated by comparison to the least squares optimization method. The centroid method is computationally more efficient than the optimization method and avoids convergence problems. In addition, its main advantage is that the permittivity or propagation velocity of the breast have not to be known beforehand. Good agreement between the two methods is obtained experimentally.

ACKNOWLEDGMENT

REFERENCES

1. Fear, E. C., J. Sill, and M. A. Stuchly, "Experimental feasibility study of confocal microwave imaging for breast tumor detection," *IEEE Transactions on Microwave Theory and Techniques*, Vol. 51, No. 3, 887–892, 2003.

2. Sill, J. M. and E. C. Fear, "Tissue sensing adaptive radar for breast cancer detection — Experimental investigation of simple tumor models," *IEEE Transactions on Microwave Theory and Techniques*, Vol. 53, No. 11, 3312–3319, 2005.

3. Klemm, M., I. Craddock, J. Leendertz, A. Preece, and R. Benjamin, "Experimental and clinical results of breast cancer detection using UWB microwave radar," *IEEE Antennas and Propagation Society International Symposium*, 1–4, 2008.

4. Craddock, I. J., M. Klemm, J. Leendertz, A. W. Preece, and R. Benjamin, "An improved hemispeherical antenna array design for breast imaging," *Proceedings European Conference on Antennas and Propagation*, 1–5, 2007.

5. Lazaro, A., D. Girbau, and R. Villarino, "Simulated and experimenal investigation of microwave imaging using UWB," *Progress In Electromagnetics Research*, Vol. 94, 263–280, 2009.

6. Bolomey, J. C., A. Izadnegahdar, L. Jofre, C. Pichot, G. Peronnet, and M. Solaimani, "Microwave diffraction tomography for

biomedical applications," *IEEE Transactions on Microwave Theory and Techniques*, Vol. 30, No. 11, 1998–2000, 1982.

7. Meaney, P. M., M. W. Fanning, D. Li, S. P. Poplack, and K. D. Paulsen, "A clinical prototype for active microwave imaging of the breast," *IEEE Transactions on Microwave Theory and Techniques*, Vol. 48, No. 11, 1841–1853, 2000.

8. Semenov, S. Y., R. H. Svenson, A. E. Boulyshev, A. E. Souvorov, A. G. Nazarov, Y. Sizov, V. Posukh, A. Pavlovsky, P. Repin, A. Starostin, B. Voinov, M. Taran, G. Tatsis, and V. Baranov, "Three-dimensional microwave tomography: Initial experimental imaging of animals," *IEEE Trans. Biomed. Eng.*, Vol. 49, No. 1, 55–63, January 2002.

9. Kosmas, P. and C. M. Rappaport, "FDTD-based time reversal approach for microwave breast cancer detection — Localization in three dimensions," *IEEE Transactions on Microwave Theory and Techniques*, Vol. 54, No. 4, 1921–1927, June 2006.

10. Lazaro, A., D. Girbau, and R. Villarino, "Wavelet-based breast tumor localization technique using a UWB radar," *Progress In Electromagnetics Research*, Vol. 98, 75–95, 2009.

11. Fontana, R. J., "Recent system applications of short-pulse ultra-wideband (UWB) technology," *IEEE Transactions on Microwave Theory and Techniques*, Vol. 52, No. 9, 2087–2104, September 2004.

12. Chen, Y., E. Gunawan, K. S. Low, S. C. Wang, Y. Kim, and C. B. Soh, "Pulse design for time reversal method as applied to ultrawideband microwave breast cancer detection: A two-dimensional analysis," *IEEE Trans. Antennas Propag.*, Vol. 55, 194–204, 2007.

13. Yang, F. and A. S. Mohan, "Ultra wideband microwave imaging and localization for breast cancer," *IEEE Microwave Conference, APMC*, 1–4, Asia-Pacific, 2008.

14. Sahinoglu, Z., S. Gezici, and I. Guvenc, *Ultra-wideband Positioning Systems*, Cambridge University Press, 2008.

15. Knapp, C. and G. Carter, "The generalized correlation method for estimation of time delay," *IEEE Trans. Acoust., Speech, and Sig. Processing (ICASSP)*, Vol. 24, 320–327, 1976.

16. Bindu, G., A. Lonappan, V. Thomas, C. K. Aanandan, and K. T. Mathew, "Dielectric studies of corn syrup for applications in microwave breast imaging," *Progress In Electromagnetics Research*, Vol. 59, 175–186, 2006.

17. Lazenik, M., D. Popovic, L. McCartney, C. B. Watkins,

M. J. Lindstrom, J. Harter, S. Sewall, T. Ogilvie, A. Magliocco, T. M. Breslin, W. Temple, D. Mew, J. H. Booske, M. Okoniewski, and S. C. Hagness, "A large-scale study of the ultrawideband microwave dielectric properties of normal breast tissue obtained from cancer surgeries," *Phys. Med. Biol.*, Vol. 52, No. 10, 6093–6115, October 2007.

18. Goswami, J. C. and A. K. Chan, *Fundamentals of Wavelets, Theory, Algorithms, and Applications*, John Wiley & Sons, Inc., 1999.

19. Li, H. J. and K. M. Li, "Application of wavelet transform in target identification," *Progress In Electromagnetics Research*, Vol. 12, 57–73, 1996.

20. Pourvoyeur, K., A. Stelzer, G. Ossberge, T. Buchegger, and M. Pichle, "Wavelet-based impulse reconstruction in UWB-radar," *IEEE MTT-S Digest*, 603–606, 2003.

21. Aly, O. A. M. and A. S. Omar, "Detection and localization of RF radar pulses in noise environments using wavelet packet transform and higher order statistics," *Progress In Electromagnetics Research*, Vol. 58, 301–317, 2006.

22. Bulusu, N., J. Heidemann, and D. Estrin., "GPS-less low cost outdoor localization for very small devices," *IEEE Personal Communications*, Vol. 7, No. 5, 28–34, 2000.

23. Reichenbach, F. and D. Timmermann, "Indoor localization with low complexity in wireless sensor networks," *IEEE Int. Conf. on Industrial Infromatics*, 1018–1023, 2006.

24. Winters, D. W., J. D. Shea, E. L. Madsen, G. R. Frank, B. D. Van Veen, and S. C. Hagness, "Estimating the breast surface using UWB microwave monostatic backscatter measurements," *IEEE Trans. On Biomedical Eng.*, Vol. 55, No. 1, 247–256, 2008.

25. Lazaro, A., D. Girbau, and R. Villarino, "Analysis of vital signs monitoring using an IR-UWB radar," *Progress In Electromagnetics Research*, Vol. 100, 265–284, 2010.

26. Li, X., S. K. Davis, S. C. Hagness, D. W. Van Der Weide, and B. D. Van Veen, "Microwave imaging via space-time beamforming: Experimental investigation of tumor detection in multi-layer breast phantoms," *IEEE Transactions on Microwave Theory and Techniques*, Vol. 52, No. 8, 1856–1865, August 2004.

27. Lai, J. C. Y., C. B. Soh, E. Gunawan, and K. S. Low, "Homogeneous and heterogeneous breast phantoms for ultra-wideband microwave imaging applications," *Progress In Electromagnetics Research*, Vol. 100, 397–415, 2010.